Optical Landau damping

M. N. Shneider
Department of Mechanical and Aerospace Engineering, Princeton University, Princeton, New Jersey 08544, USA

P. F. Barker
The Department of Physics, School of Engineering and Physical Sciences, Heriott-Watt University, Edinburgh EH14 4AS, Scotland
(Received 12 November 2004; published 10 May 2005)

We study the transfer of energy from an optical potential to atomic and molecular gases and demonstrate that this process is analogous to collisionless Landau damping of electrostatic potentials in plasmas and gravitational potentials observed on astrophysical scales. We show that a signficant fraction of the light attenuation within a cavity can be attributed to this mechanism when the cavity is filled with a gas at high density. The resulting motion of particles created by optical Landau damping can be used to induce transport when a periodic potential produced by two counterpropagating high-intensity pulsed optical fields is used. Bulk drift of the gas also appears feasible even when the mean kinetic energy is much greater that the maximum optical potential.

DOI: 10.1103/PhysRevA.71.053403 PACS number(s): 32.80.Lg, 51.10.+y, 02.30.Jr

Landau damping [1] is an important mechanism for dissipation in a wide range of collisionless systems in plasma science [2,3], astrophysics [4,5], and low-temperature physics [6]. In this process, energy is transferred from a traveling potential to the system in the absence of collisions, resulting in a damping of the original potential wave. In a collisionless plasma, Landau damping of an electrostatic wave created by a periodic disturbance is damped by the interactions between the charged particles and the electrostatic wave. The resulting asymmetry induced in the Maxwell-Boltzmann distribution results in a bulk drift and rapid damping of the electrostatic wave. In astrophysical systems, the damping of a gravitational potential is induced by gravitional attraction. For all cases, a generalized potential traveling in the system will trap particles that are traveling close to the phase velocity, ξ, of the potential. In the absence of collisions, particles moving at the phase velocity of the potential, and in phase with the trough of the potential, will experience no force and travel with the potential. Particles that are moving slightly slower or faster than the phase velocity will be trapped, if their kinetic energy, as measured in the reference frame of the traveling wave, is less than or equal to the well potential energy. These particles will have velocities in the range $v=\xi\pm\Delta$, where $\Delta=\sqrt{2\phi_m/M}$, ϕ_m is the potential well depth, and M is the mass of the particles. The trapping process increases the mean velocity of slower particles and decreases that of the faster particles, creating a plateau $[\partial f(v)/\partial v=0]$ in the distribution function $f(v)$ centered at the phase velocity of the traveling wave of a thermally distributed system of particles [2,3]. This process transfers energy from the potential to the system of particles, and in the case of strong interactions, significantly attenuates the potential by collisionless Landau damping and induces bulk motion in the system [7].

Conservative optical potentials have been used extensively to trap and manipulate ultracold atoms in the nK to μK range using the optical dipole force [8–14]. Larger potentials in the 100 K range can be produced by high-intensity pulsed lasers for shorter time periods [15]. These stronger potentials have been used to deflect cold molecules (5 K) and, more recently, to dissociate diatomic molecules by strong centrifugal optical forcing [16,17].

In this paper, we demonstrate that an optical periodic potential created by the interaction between a light field and the polarizability of a neutral atom or molecule can undergo an analogous process to Landau damping, which we call optical Landau damping. In this process, the dissipation of the optical wave is transformed into particle motion via the dipole force. We begin by demonstrating that the motion of a thermal ensemble of particles can be strongly perturbed by an optical potential when the mean kinetic energy is less the potential well depth, and like Landau damping in other systems, it leads to transport and bulk motion. We then study the damping of the optical potential within a cavity containing a gas at high densities and predict that this phenomenon would be observed in the temporal decay of the optical field within the cavity. Finally, we consider bulk drift and fluidic processes induced in a capillary by weak (mK) CW optical potentials.

I. OPTICAL LANDAU DAMPING IN A PERIODIC OPTICAL POTENTIAL

We consider the forces on atoms or molecules within a one-dimensional periodic optical dipole potential created by the interference of two counterpropagating fields with wave vectors $\vec{k}_1$ and $\vec{k}_2$. In atomic and molecular optics, this is often called an optical lattice. Figure 1 is a schematic diagram of a lattice created by two optical fields E_1 and E_2 and with frequencies ω_1 and ω_2. The phase velocity of the traveling potential is given by $\xi=\Delta\omega/q$, where the wave number $q=|\vec{k}_1-\vec{k}_2|=k_1+k_2$ and the angular difference frequency between the two fields is $\Delta\omega=\omega_1-\omega_2$. For an atom with a traveling wave field created by two fields that are far from resonance, the potential is well approximated by the quasielectrostatic expression [18]

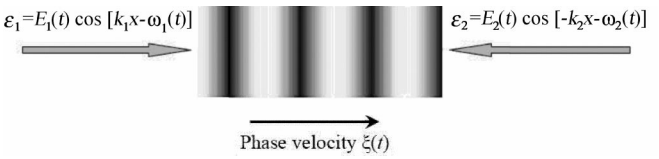

FIG. 1. The creation of an optical lattice by two counterpropagating optical fields. The frequency difference between the two beams determines the speed of the lattices.

$$\phi(x,t) = \tfrac{1}{2}\alpha E(x,t)^2, \tag{1}$$

where α is the effective polarizability of the particle and $E(x,t)$ is the electric field of the optical waves. We study the classical motion of particles in large potentials in the 1–100 K range that can be created by pulsed optical fields far from resonance. The classical motion of molecules within constant velocity optical lattices created by two counterpropagating fields has been measured [19], and the motion in accelerating potentials has been predicted [20–22]. The demonstration of important statistical mechanical phenomena and the quantum-mechanical motion of cold atoms in optical lattices using potentials in the μK range have been investigated both experimentally and theoretically [12,13]. For two counterpropagating laser beams with intensity $I=I_1+I_2$, the maximum potential well depth is $\phi_m=\alpha I Z_0/n$, where $Z_0=\sqrt{\mu_0/\varepsilon_0}=376.73\ \Omega$ and n is the index of refraction.

To study the time- and space-dependent motion imparted to a thermal distribution function, $f=f(x,v,t)$, of polarizable particles by a one-dimensional (1D) optical potential (1), we solve the one-dimensional Boltzmann equation with the Bhatnagar, Gross, and Krook (BGK) collision integral approximation [23],

$$\frac{\partial f}{\partial t} + v\frac{\partial f}{\partial x} - \frac{\nabla\phi(x,t)}{M}\frac{\partial f}{\partial v} = -\frac{f-f_0}{\tau_{\mathrm{col}}}, \tag{2}$$

where f_0 is the MB velocity distribution. The relaxation time in the BGK collision integral approximation is given by $\tau_{\mathrm{col}}=l_c/v_m$, where $l_c=1/\sqrt{2}\pi d^2 N$ is the free collision length for gas with density N and particles with diameter d, and $v_m=\sqrt{8k_bT/\pi M}$ is the mean velocity. We consider perturbations to the distribution function of a gas of argon which is initially at 300 K, and in thermal equilibrium at a pressure of 0.01 Torr. The fields used to form the optical potential have a maximum field intensity of 1.62×10^{12} W/m^2 which corresponds to an average potential well depth of 78.1 K. We seek particular solutions to the Boltzmann equation by assuming that the potential is created by pulsed laser fields with a Gaussian temporal profile with a full width at half maximum (FWHM) of 10 ns. A periodic potential with infinite length allows the use of a cyclic boundary condition $\delta f(-L/2,v,t)=\delta f(L/2,v,t)$, where $L=2\lambda$, and $\lambda=4\pi/q$ is subject to the boundary conditions $f(x,v\to\pm\infty,t)=0$. This will correctly model the motion along the axis for a large proportion of the particles. To calculate the distribution function, Eq. (2) is numerically integrated using a MacCormack finite-difference scheme [24], with a zero initial condition, $f(x,v,0)=f_0$, where f_0 is the 1D Maxwell-Boltzmann function for the gas at the initial gas temperature.

Figure 2 shows the evolution of the velocity distribution function calculated for the optical potential traveling at 316.3 m/s at different times during the 10 ns pulse. As the potential has a periodicity of half a wavelength, the distribution function is averaged over this scale. As shown by the perturbation to the velocity distribution function, the potential is capable of trapping atoms centered at 316.3 m/s with an average velocity spread of 180 m/s as shown by the width of the perturbation. The asymmetry induced in the distribution function implies that a localized bulk velocity will be induced in the gas at this time and also that the optical potential must be damped since energy must be expended in producing the plateau.

The modification to the velocity distribution functions, as shown in Fig. 2, are due to particles that are trapped by the potential, but also to untrapped particles that are strongly perturbed by the moving potential. The trapped particles slosh back and forth between the walls of the potential and exchange energy with it. As there are more particles at the lower velocities, more energy must be taken out of the potential until a flat plateau with a width equal to the potential well depth is formed. After this time, equal energy is given to and taken away from the potential when averaged over an oscillation cycle.

When the density is low, such that the lattice period is less than the mean free path $\lambda \ll l$, the plateau in the distribution function created by the trapped species can be used to calculate a drift velocity,

$$V_{dr}(t) = \frac{1}{N}\left\langle \int_{-\infty}^{\infty} v f(v,x,t)dv \right\rangle_{\lambda} \approx \frac{1}{N}\int_{\xi-\Delta}^{\xi+\Delta} \delta f v dv. \tag{3}$$

The corresponding density of the kinetic energy is

$$K = \left\langle \int_{-\infty}^{\infty} \frac{Mv^2}{2}[f(v,x,t)-f_0(v)]dv \right\rangle_{\lambda} \approx \int_{\xi-\Delta}^{\xi+\Delta} \frac{Mv^2}{2}\delta f dv, \tag{4}$$

where N is the number density and δf is the difference between the temporally or spatially averaged velocity distribution function $f(v)$, which results from the traveling periodic potential, and the MB distribution function, $f_0(v)$ corresponding to thermal equilibrium. We only consider particles with velocities in the $\xi\pm\Delta$ velocity range to be significantly perturbed by the potential. The difference δf is approximated by Taylor expansions of the functions $f(v)$ and $f_0(v)$ centered at the phase velocity of the potential, assuming an idealized plateau [2,3] where $f(v)=f_0(\xi)$ and where $\partial f(v)/\partial v=0$ in the region $\xi\pm\Delta$. The difference to first order is given by $\delta f(v)=f(v)-f_0(v)\approx-[\partial f_0(v)/\partial v]_{\xi}\delta v$, where $\delta v=v-\xi$. From Eq. (3), the drift velocity is given by

$$V_{dr} = \frac{2}{3}\Delta^3 f_0(\xi)\frac{M\xi}{Nk_bT}, \tag{5}$$

and from Eq. (4) the density of kinetic energy

$$K = \frac{2}{3}\frac{M^2 f_0(\xi)\xi^2\Delta^3}{k_bT} = NMV_{dr}\xi. \tag{6}$$

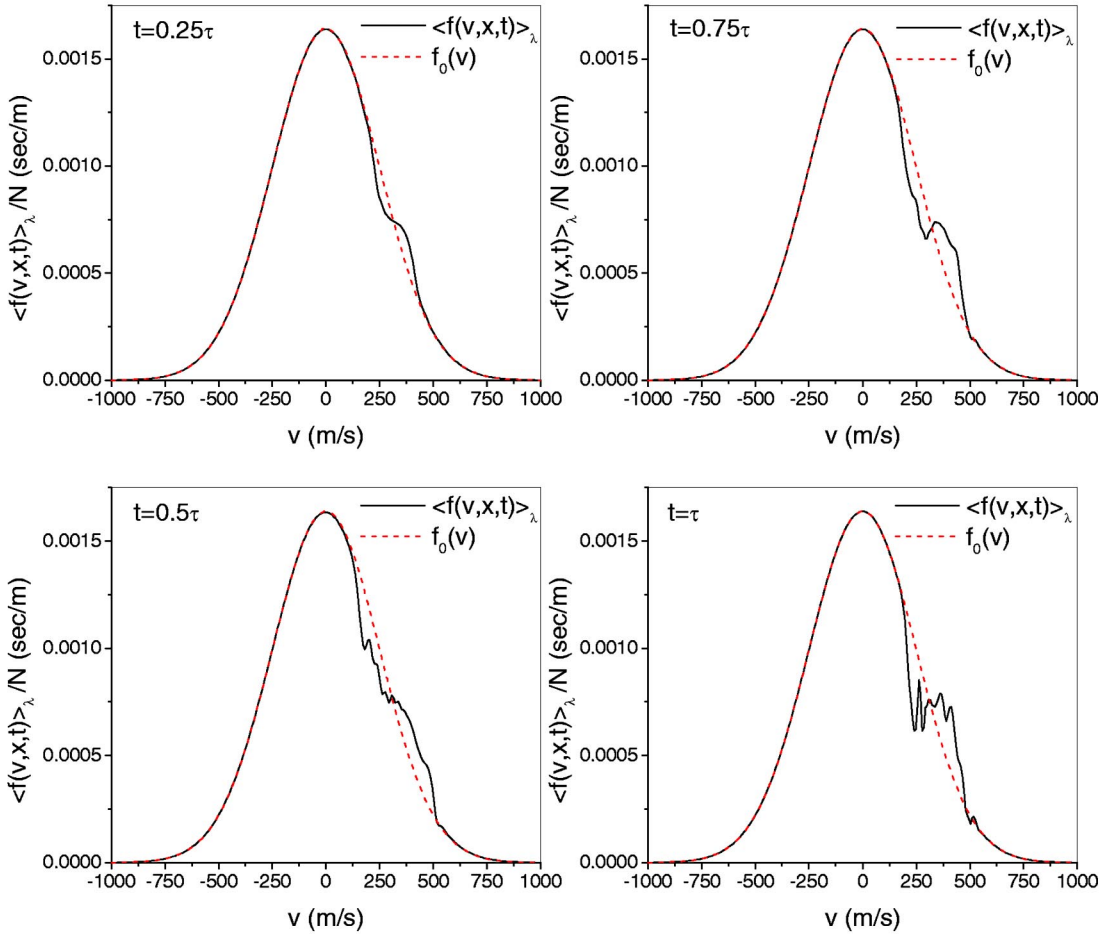

FIG. 2. The evolution of a perturbation to the velocity distribution function of argon gas at 0.01 Torr and 300 K by a moving pulsed optical lattice. The dotted line is the unperturbed distribution function in the absence of the optical fields. The laser intensity is $I_a = 1.62 \times 10^{16}$ W/m^2, which corresponds to a potential well depth of 78.1 K; $\lambda = 795$ nm.

From Eq. (5) it follows that a maximum drift, $V_{dr}^{\max} \approx 0.161/k_B T\,((2\phi_m)^3/M)^{1/2}$, can be achieved when the traveling wave velocity equals $\xi = \sqrt{k_B T/M}$. For instance, in argon at a temperature of 300 K and a potential well depth of 78.1 K (corresponding laser beams intensity, $I_a = 1.62 \times 10^{16}$ W/m^2), a maximum drift velocity of 15.1 m/s is estimated at $\xi \approx 250$ m/s. From Eq. (6) it follows that a maximum density of kinetic energy reaches when $\xi = \sqrt{2k_B T/M}$.

To quantifiy how much energy from the optical potential is damped by this type of motion, we can calculate the rate of dissipation of kinetic energy K as $dW/dt = -K/\tau_{\rm col}$, where $\tau_{\rm col}$ is relaxation time or average time between the collisions. When the phase velocity is given by $\xi = \sqrt{2k_B T/M}$, the energy density is given from Eq. (6) by $K = \frac{4}{3} M f_0(\xi)\Delta^3 \approx \frac{4}{3} n_{well}\phi_m$, where the number density of particles in the optical potential is $n_{well} = \int_{\xi-\Delta}^{\xi+\Delta} f(v)dv \approx 2 f_0(\xi)\Delta$, and the power dissipated therefore scales as

$$\frac{dW}{dt} \approx -\frac{4}{3}\frac{n_{well}\phi_m}{\tau_{\rm col}}. \tag{7}$$

The optical power dissipated can be calculated more accurately at any density from the bulk drift velocity induced by the optical potential determined by numerical integration of the Boltzmann equation. The corresponding local velocity of the gas, calculated from the distribution function perturbed by the lattice as $V(x,t) = (1/N)\int f(x,v,t)v dv$, is shown below in Fig. 3. To understand how this bulk drift increases during the pulse duration, we calculate this value as a function of time by averaging Eq. (3) over the periodicity of the velocity perturbation using the same potential as observed on Figs. 3(a)–3(d). At each time corresponding to a fraction of the Gaussian pulse width τ (defined to be twice the FWHM), the velocity is always periodic, but most importantly, the average velocity in each figure is greater than zero and increases with time in the absence of collisions.

Figure 4(a) shows the evolution of the drift velocity calculated from

$$\langle V(x,t)\rangle_\lambda = \frac{1}{N\lambda}\int_0^\lambda \int_{-\infty}^{\infty} f(x,v,t)v dv dx, \tag{8}$$

during a pulse with a Gaussian temporal profile for three potentials with the same well depth and phase velocity (316 m/s), but with different spatial periods of 397 nm, 795 nm, and 1.59 μm. In each case, the maximum drift is

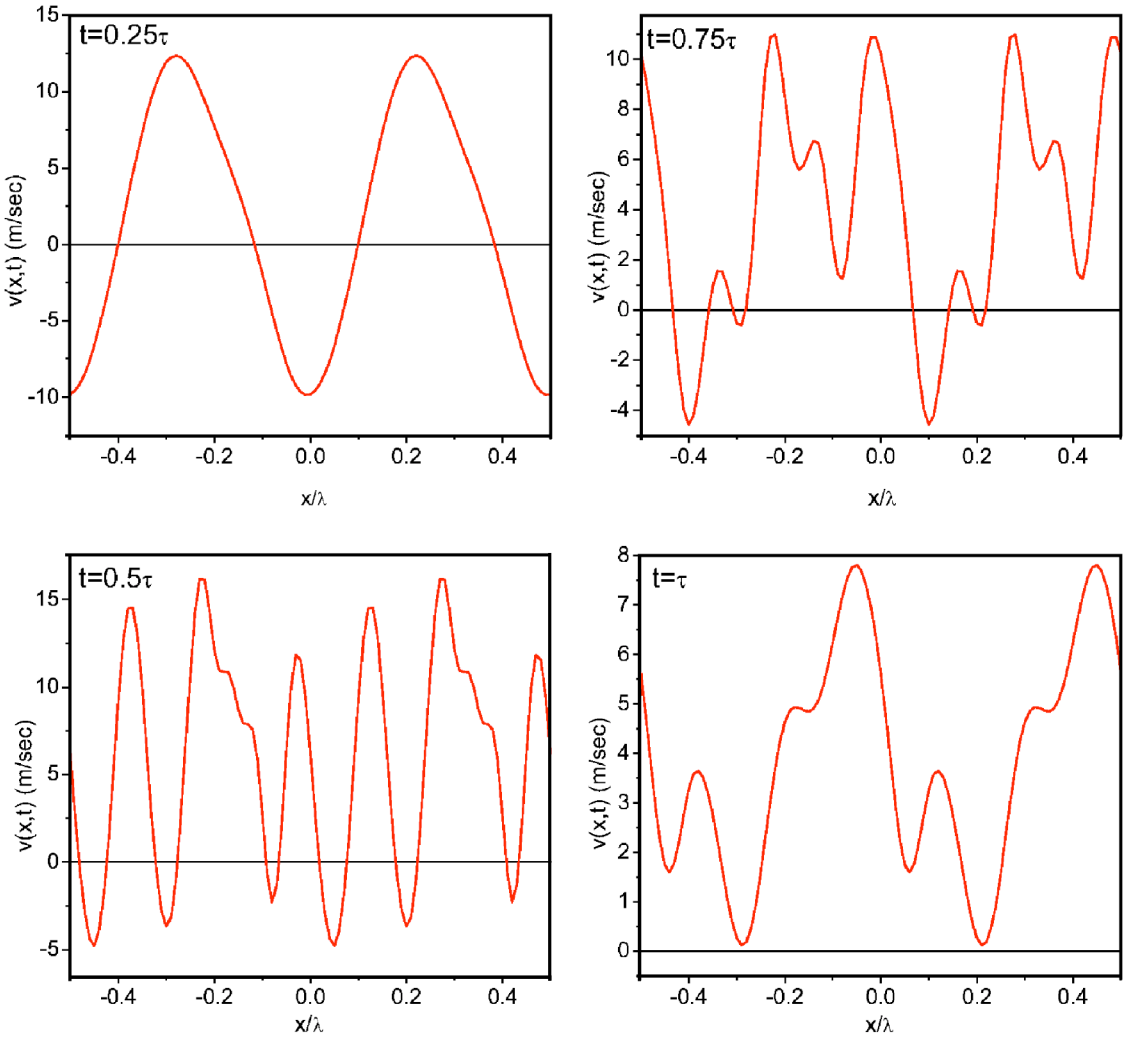

FIG. 3. Local gas velocity $V(x,t)$ within the lattice as different times during the laser pulse. The pulse conditions are the same as in Fig. 2.

induced when the potential is greatest in the middle of the pulse. Bulk drift implies that a net momentum has been imparted to the gas from the optical fields and therefore that Landau damping of the optical potential will occur during the pulse. To quantify this, we calculate the instantaneous power per unit volume imparted to the gas from the potential as a function of time given by

$$\langle P(x,t)\rangle_\lambda = \frac{1}{\lambda}\int_0^\lambda \int_{-\infty}^{+\infty} [-\nabla \phi(x,t)] v f(x,v,t) dv dx. \quad (9)$$

Figure 4(b) is a plot of the power transferred to the gas by the optical potential with three spatial different periods as in Fig. 4(a). In each case, the power fluctuates with a well defined period, which for the shortest period potential is approximately 2.6 ns for $\Delta\omega = 10^{10}$ rad/s and 5.2 for $\Delta\omega = 2.5 \times 10^9$ rad/s. These oscillations are due to particles oscillating between the two walls of the potential.

The dissipated power and drift velocity averaged over a spatial period as a function of the optical lattice frequency difference $\Delta\omega = \omega_1 - \omega_2$ is shown in Fig. 5. The gas and optical pulse conditions are the same as used in the previous figures.

In the initial part of the laser pulse, power is absorbed by the particles $[\langle P(x,t)\rangle_\lambda > 0]$, but by the end of the pulse, power is transferred back into the optical potential $[\langle P(x,t)\rangle_\lambda < 0]$. The total kinetic energy gained by the gas, and lost from the optical potential, at the end of the pulse is $\Delta E = \langle K(x,t)\rangle_\lambda \pi r_b^2 L_{OL}$, where r_b is the laser beam effective radius and L_{OL} is an effective optical lattice length.

For a peak laser intensity of $I_a = 1.62 \times 10^{12}$ W/cm^2 with Gaussian pulse duration $\tau = 20$ ns (FWHM = 10 ns) and interaction length of $L_{OL} \sim 1$ cm, the ratio of dissipated energy to the total energy radiated by the lasers per pulse is $\Delta E_L = \pi r_b^2 \int_0^\tau I(t) dt$ and $\Delta E / \Delta E_L \sim 10^{-12}$. So although the distribution function, and therefore the momentum of the particles, can be signficantly modified by the large optical potential, the dissipation of laser energy is negligibly small and not observable in this type of experiment.

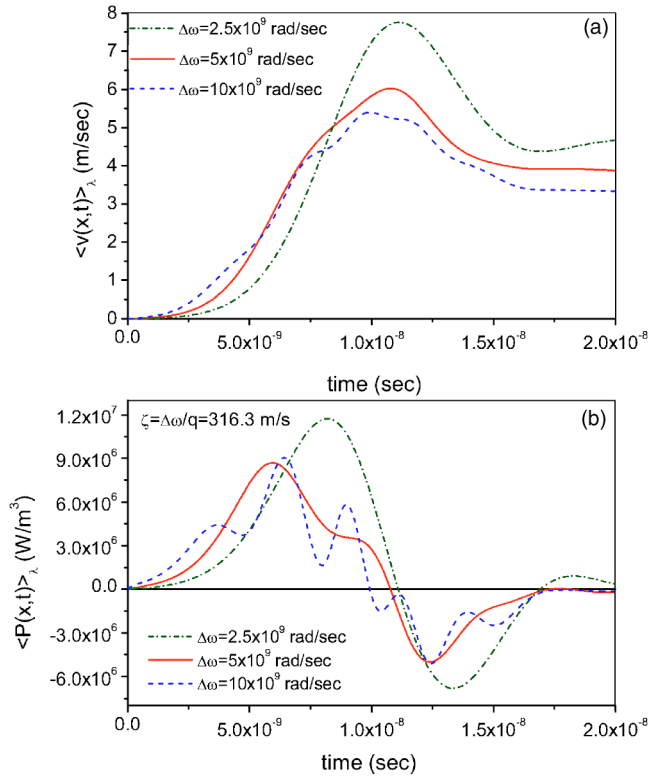

FIG. 4. (a) Plots of the drift velocity as a function of time during the laser pulse. (b) Plots of the power dissipated by the mechanical motion of the atoms within the lattice at phase velocity $\xi = 316.3$ m/s for different optical lattice wavelengths. Gas conditions and pulse parameters are the same as in Fig. 2.

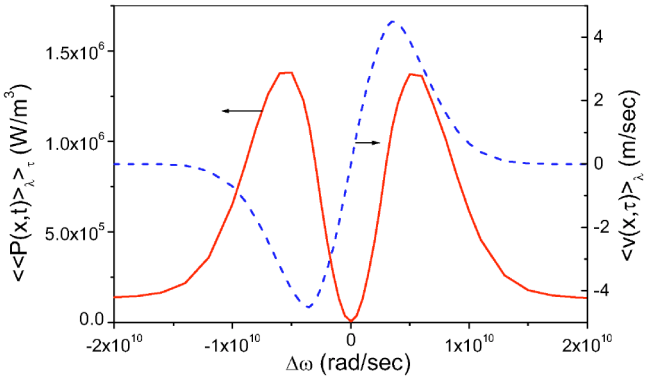

FIG. 5. The averaged dissipated power per laser pulse, $\langle\langle P(x,t)\rangle_\lambda\rangle_\tau$, and the drift velocity, $\langle\langle V(x,t)\rangle_\lambda\rangle_\tau$, at different $\Delta\omega$. Gas conditions and pulse parameters are the same as in Fig. 2.

II. OPTICAL LANDAU DAMPING IN A CAVITY

Although the large changes to the velocity distribution function can be made using high-intensity fields as discussed above, the power dissipated for a single laser pulse is relatively small. The damping of the optical field may, however, be observed by amplifying the attenuation of the optical potential by multiple passes of both lattice beams through the interaction region and by increasing the density of the particles within the potential. This may be observed within an optical cavity such as that used for cavity ringdown spectroscopy, where the decay of the intensity of light transmitted through the mirrors is used to measure an effective light loss usually due to absorption. For this type of experiment, the temporal variation in intensity of a pulsed field in this type of cavity is given by

$$dI/dt = -I/\tau_Q - N\sigma_R Ic - 2P_d cl/L_M. \tag{10}$$

In this expression, the empty cavity liftime is $\tau_Q = L_M/[c(1-R)]$, and L_M is the distance between the mirrors, R is the reflectivity, and l is the interaction region length in which the intensity is high enough to induce optical damping. In the absence of absorption, the only other loss besides optical Landau damping is Rayleigh scattering (which has a cross section [18] $\sigma_R = 8\pi^3\alpha^2/3\varepsilon_0^2\lambda^4$), proportional to the density of molecules N. P_d is the power absorbed due to Landau damping of one of the lattice beams that is formed within the cavity by the two counterpropagating beams. We assume that the density is so high within the cavity that particles collide with other particles before they reach the other side of the potential. The typical time for a collision between a particle and the potential is given by $\tau_{\rm col} = l_c/|v - \xi|$, where ξ is the lattice phase velocity. We therefore consider the situation where the mean free path is smaller than the period of the optical lattice potenial ($l_c \ll \lambda$).

In a single collision where the walls of the potential are moving, the change in kinetic energy is given by $\Delta\varpi = 2M(v-\xi)\xi$ and therefore the power transferred per particle to the wall is $\Delta\dot{\varpi} = \Delta\varpi/\tau_{\rm col} = 2M(v-\xi)^2\xi/l_c$. The total rate of gas energy exchange (or optical lattice energy dissipation) is given by

$$\frac{dW}{dt} = \frac{2M\xi}{l_c}\left[\int_\xi^{\xi+\Delta}(v-\xi)^2 f(v)dv - \int_{\xi-\Delta}^{\xi}(v-\xi)^2 f(v)dv\right].$$

We can estimate these integrals by expanding the distribution function as a Taylor series to first order $f(v) \approx f_0(\xi) + (df_0/dv\xi)(v-\xi)$ The total disspation rate is given by

$$\frac{dW}{dt} = \frac{M\xi}{l_c}\frac{df_0}{dv_\xi}\Delta^4,$$

where $\Delta = \sqrt{2\phi_m/M}$, $\phi_m = \alpha I z_0$ is the potential well depth, and $z_0 = \sqrt{\mu_0/\varepsilon_0} = 376.7\ \Omega$ is the impedance of free space.

For a Maxwellian distribution function, $(df_0/dv)_\xi = -(M\xi/kT)f_0(\xi)$, the dissipation rate is given by

$$\frac{dW}{dt} = -\frac{M^2\xi^2}{l_c k_B T} f_0(\xi)\Delta^4. \tag{11}$$

The power absorbed by the gas, P_d, due to the optical wave dissipation is $P_d = -dW/dt$ and the energy density of an electromagnetic wave is $W = \varepsilon_0 E_a^2/2 = I/c$. It then follows by substitution in Eq. (11) that $dI/dt = -(4\xi^2/l_c k_B T) f_0(\xi)\phi_m^2 c = -\theta(\xi)I^2$, where $\theta(\xi) = (2\xi\alpha z_0)^2 f_0(\xi)c/l_c k_B T$. For the initial condition $I(0) = I_0$, the intensity at any later time within the cavity is given by

$$I = \frac{I_0}{1 + \theta I_0 t}.$$

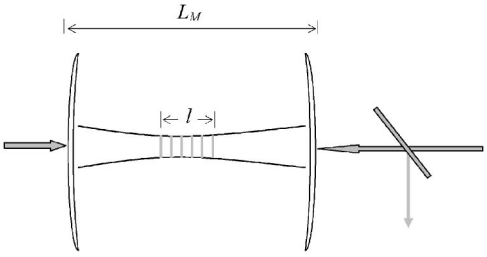

FIG. 6. Diagram of an experimental arrangement to measure optical Landau damping within a near-concentric optical cavity. Optical fields are introduced into both mirrors to create two traveling optical potentials.

We can find a phase velocity which corresponds to the maximum dissipation rate when $\theta(\xi)'=0$ at $\xi_{\max}=\sqrt{2k_BT/M}$. This corresponds to a frequency difference of $\Delta\omega_{\max}=(4\pi/\lambda)\xi_{\max}$, which for Ar gas at a temperature of 300 K gives a lattice velocity of $\xi_{\max}=353$ m/s and an angular frequency difference of $\Delta\omega_{\max}=4.2\times10^9$ rad/s. Note that there is no optical Landau damping when the lattice velocity is equal to zero. This is because particles colliding with the potential wall on average return as much energy as they take from it.

By substituting the expression for the power dissipated (the optical Landau damping rate) for a Maxwellian distribution into the cavity decay of Eq. (10), we can determine how optical Landau damping will modify the decay of the field within a cavity. At present, the best reflectivity for commercial mirrors is given by $R=0.999\,99$ [25]. To model the optical damping, we have used a much lower reflectivity $R=0.999\,95$ that is commonly available for cavity ringdown applications [26]. We have kept the initial laser beam intensity in the intersection region $I_0=5\times10^8$ W/cm^2 lower where a breakdown in gases by pulsed laser radiation occurs [27]. A stable near-concentric cavity will be required to maintain a small beam waist (60 μm) over a long Rayleigh range (interaction region length, $l=2.5$ cm, $L_M=50$ cm (Fig. 6).

We investigate damping in the cavity by plotting the transmitted intensity out of the cavity as a function of time. We have simulated this decay for a cavity containing argon at a pressure of 50 atm and a temperature of 20 degrees celsius. The Rayleigh range was used as the effective interaction length over which damping would occur. Figure 7 shows the exponential decay of light for the case of no LD with only Rayleigh scattering and mirror losses and the dotted curves indicate how this decay varies with the speed of the lattice within the cavity (at different $\Delta\omega=|\omega_2-\omega_1|$)). We estimate the temperature rise as $\Delta T\sim(2/NMc_v)\int_0^\infty P_d(t)dt$, where $c_v=320$ J/kg K is a specific-heat capacity of argon at constant volume. At 50 atm, the temperature increases in the interaction region by $\sim$3.9 K. As this is a relatively small perturbation on the 300 K temperature of the gas, our predictions using a Gaussian distribution at 300 K will not be significantly modified.

The relative role of each cavity decay mechanism in Eq. (10) at 50 atm and different $\Delta\omega$ is shown in Fig. 8.

The dependence of the characteristic decay time (the time when intensity in the cavity drops in e times) on gas pressure

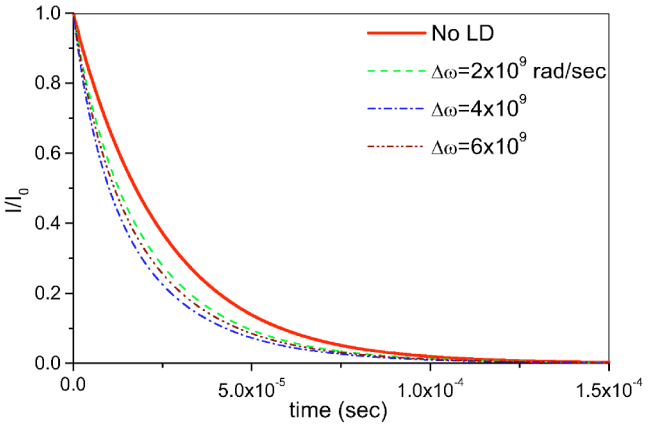

FIG. 7. Laser intensity as a function of time in the cavity with and without Landau damping for argon at a temperature of 293 K at a pressure 50 atm. The laser intensity was $I_0=5\times10^{12}$ W/m^2 using cavity mirrors of reflectivity $R=0.999\,95$; $\lambda=1064$ nm.

at the same cavity and laser beam parameters is shown in Fig. 9. At 50 atm, a maximum change in the decay rate of 63% occurs when there is a frequency difference of 665 MHz between the two beams in the cavity. This corresponds to a lattice velocity of 354 m/s, which is very close to the above estimations of $\Delta\omega_{\max}$ and $\xi_{\max}$. We do not consider the excitation of acoustic waves by the traveling optical potential within the cavity. At the pressure we have considered (50 atm), dissipation by this mechanism may be greater than that predicted in our treatment and would require further study.

III. LANDAU DAMPING WITH CONTINUOUS WAVE (CW) OPTICAL FIELDS

Large potentials can be created by pulsed fields far from resonance, but the effects of optical Landau damping may also be observed using smaller CW fields when they are tuned close to a strong atomic resonance. Here dipole potentials in the 1 mK range can be created and are capable of inducing perturbations in colder gases.

For a two-level atom in a traveling wave field (Fig. 1) with a constant phase velocity, this optical potential is given by [28]

$$\phi(x,t)=\frac{1}{2}\hbar\delta\ln\left[\frac{1+2s_0[\cos(qx-\Delta\omega t)+1]+(2\delta/\gamma)^2}{1+(2\delta/\gamma)^2}\right], \tag{12}$$

where δ is the detuning of the laser beams from resonance, γ is the natural linewidth, and $s_0=I/I_s$ is the on-resonance saturation parameter given by the laser intensity, I, and saturation intensity, I_s. We are interested in the regime where the laser is detuned far from resonance, and where the saturation parameter $s=4s_0\cos^2(qx-\Delta\omega t)/[1+(2\delta/\gamma)^2]\ll1$. In this regime, there are essentially no velocity-dependent forces. It is important that there is a neglible probability for atoms to exist in the excited state because they will experience a force that is π out of phase with ground-state atoms. In this case,

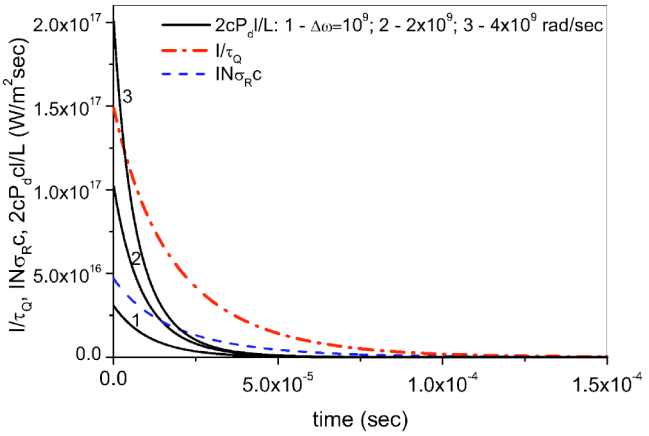

FIG. 8. The intensity as a function of three laser detunings illustrating the effect of optical Landau damping in the cavity. Also shown is empty cavity decay in the absence of other loss mechanisms and the contribution to the cavity decay by Rayleigh scattering.

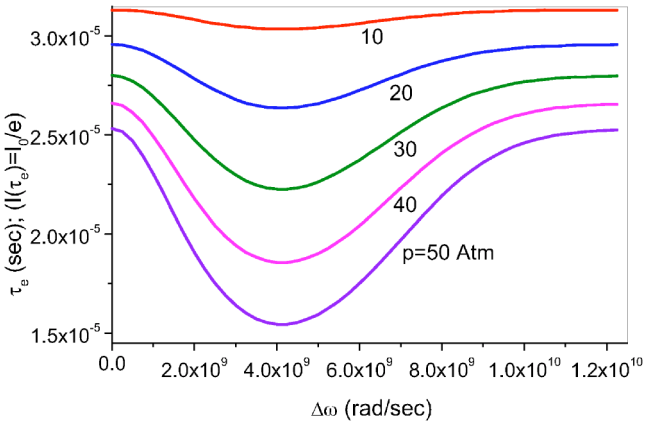

FIG. 9. Characteristic decay time in the cavity vs $\Delta\omega$ at different gas pressure. Cavity and laser parameters are the same as in Fig. 7.

the force on the particles will spatially average to zero when operating close to saturation because atoms rapidly cycle at the Rabi frequency between the excited and ground state. The dipole force on a two-level atom ensemble for a traveling wave at $\xi=\Delta\omega/q$ is given by [28]

$$F(x,t) = -\nabla\phi(x,t) = \frac{2\hbar k\delta s_0 \sin(qx-\Delta\omega t)}{1+2s_0[\cos(qx-\Delta\omega t)+1]+(2\delta/\gamma)^2}$$

$$\approx q\frac{\hbar\gamma^2}{4\delta}s_0\sin(qx-\Delta\omega t). \tag{13}$$

We can determine the time- and space-dependent motion of the gas within the optical potential from the velocity distribution function created by the external periodic dipole force. For simplicity, and to illustrate the essential physics, we solve the one-dimensional Boltzmann equation (2) with the Bhatnagar, Gross, and Krook (BGK) collision integral approximation. The dipole force for a traveling wave formed by the interference between two counterpropagating beams is given by Eq. (13).

A periodic potential with infinite length allows the use of the cyclic boundary condition $f(-L/2,v,t)=f(L/2,v,t)$, where $L=2\lambda$, and $\lambda=4\pi/q$. Equation (2) is also subject to the boundary conditions $f(x,v\rightarrow\pm\infty,t)=0$, which were numerically integrated using a McCormack finite-difference scheme [24], with an initial condition $f(x,v,t=0)=f_0(v)$.

We have chosen to model the velocity drift induced in rubidium vapor in a hollow capillary because it has been used previously for both laser guiding and LID experiments [11,29]. It also has a strong transition at 780.76 nm, which is accessible with the tunable CW Ti:sapphire laser. The vapor pressure of rubidium can be conveniently controlled by temperature. In the case we considered, the potential is created in a capillary of radius $r=20$ microns by 100 mW counterpropagating beams that are detuned approximately 80 GHz below the $5\,^2S_{1/2}-5\,^2P_{3/2}$ resonance corresponding to a potential well depth of 50 mK.

For these conditions where $s\ll 1$, and where the Rabi frequency is significantly less than the detuning, only forces on atoms in the ground state need to be considered. The radiation pressure force or dissipative force from a single beam is four orders of magnitude less than the dipole force in a traveling wave at this intensity and detuning, and therefore we do not need to consider its effect on drift [28]. Our one-dimensional analysis, which does not take into account the radial variation of intensity inside the fiber [30], will induce a radial variation in drift velocity. Although most atoms are in the ground state, a small fraction will be excited which will lead to both radial and longitudinal heating, causing atoms to be temporally lost from the periodic trapping potentials [32]. This will not prevent drift, since only a small proportion of the MB distribution must be trapped to induce transport, and a temperature rise will only reduce the effectiveness in proportion to $1/T$. In practice, this temperature rise can be controlled by collisions with the fiber walls that are maintained at a constant temperature.

The velocity distribution function, obtained from numerical solutions of Eq. (2), is shown in Fig. 10(a) for two traveling wave velocities for rubidium vapor at a temperature of 560 K and saturation pressure of 100 Pa. The traveling wave velocities of the potentials correspond to a detuning of 238.7 MHz and 478.5 MHz between the counterpropagating beams, which are both detuned approximately 80 GHz from the line center. The distribution functions were averaged over a spatial period and normalized by the number density. Equation (2) was integrated until steady state was reached. In insets in Fig. 10(a) show that in each case the center of the plateau created by the trapping potential corresponds to the phase velocity of the traveling wave. The plateau width of $2\Delta v\approx 5$ m/s is in good agreement with the simple analytical estimate of 6.3 m/s for this potential-well amplitude value.

The bulk gas velocity $V(x,t)=\int_{-\infty}^{\infty}f(x,v,t)v dv$ is periodic for all cases and oscillates with a period $T=2\pi/\Delta\omega$ at any location but gas drift velocity, $V_{dr}(t)=\langle V(x,t)\rangle_\lambda\neq 0$. The drift velocity was calculated for a range of traveling wave phase velocities by averaging the time-dependent velocity over a temporal period T at a given location, and also by averaging over a spatial period λ at a given time t. Because both kinds of averaging produce the same result, only an average over a

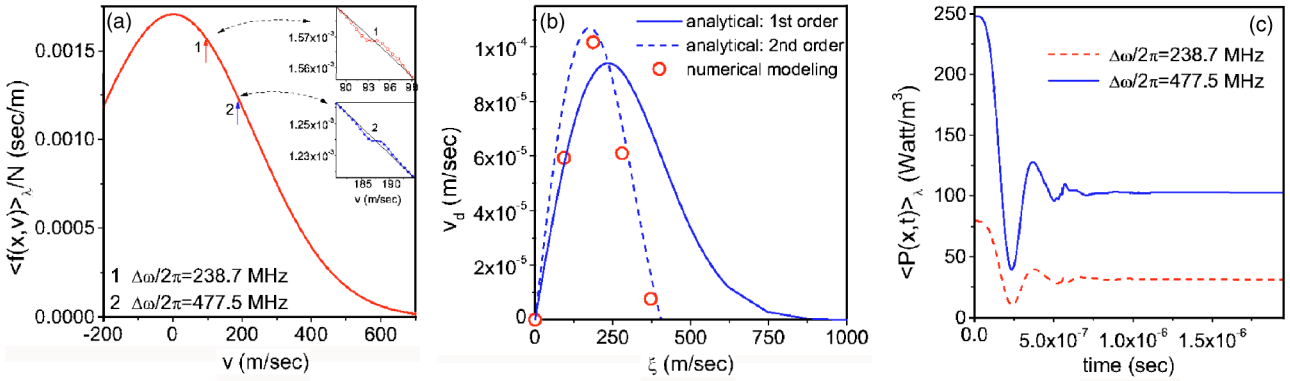

FIG. 10. (a) The normalized velocity distribution for two traveling wave velocities of 93 m/s and 186 m/s, respectively. (b) The drift velocity calculated for rubidium gas at different temperatures, as a function of traveling wave velocity. The open circles are derived from numerical modeling at 560 K and 100 Pa, and the lines are estimates of drift velocity. The dashed line corresponds to the more exact second order of Taylor expansions of the functions $f(v)$ and $f_0(v)$ [22]. (c) The average power per unit volume transferred to the gas for traveling wave velocities of 93 m/s and 186 m/s. The power transferred from the optical field to the gas results in Landau damping of the optical field.

temporal period is shown in Fig. 10(b) for a temperature of 560 K and 100 Pa. For comparison, the drift velocity estimated from Eq. (5) is shown in the same figure for the above conditions. Good agreement between the numerical predictions and the analytical estimate is shown. The average drift velocity increases with phase velocity until the number of particles that can be trapped in the MB distribution decreases faster than the increase in phase velocity. From the Eq. (5) it also follows that at lower temperatures, higher drift velocities can be accomplished because the original distribution function is narrower, allowing more particles to be trapped for a particular well depth.

The power per unit volume imparted by the optical field can be calculated from the force and induced velocity. The power averaged over the spatial period $\langle P(x,t)\rangle_\lambda$ is given by Eq. (9) and is shown in Fig. 10(c) for the two traveling wave velocities, 93 m/s and 186 m/s, at a particular spatial location. The transferred power oscillates after the field is turned on as the atoms oscillate in the potential well exchanging energy with the traveling wave. This is optical Landau damping, where atoms with velocities less than the phase velocity take energy from the field, and faster atoms give energy to the field through stimulated scattering. Because the distribution is initially Gaussian, a greater fraction of the atoms that are trapped are moving slower rather than faster than the phase velocity. As a result, net power is removed from the beam. If no collisions occur, no further average dissipation will occur. This process is equivalent to the energy dissipation of electrostatic plasma waves by collisionless Landau damping [1–3] and current drive phenomena [7]. Thus, we call the transfer of energy from the optical field to the particles, and the resulting dissipation, optical Landau damping. As shown in Fig. 10(c), the average power absorbed achieves a steady-state value $P_d=\langle P(x,t)\rangle_\lambda \approx$ const for time periods much greater than the relaxation time. The power at steady state is determined by collisions, which remove energy from the trapped particles. For conditions corresponding to presented numerical solution [Figs. 10(a) and 10(b)], the dissipation rate $P_d=K/\tau_{\mathrm{col}}$, with K defined by Eq. (6), at phase velocities $\xi=186$ and 93 m/s is $P_d\approx 156.7$ and ≈ 44.6 W/m^3, respectively. These estimations are in good agreement with numerical results, presented in Fig. 10(c).

The transport of gas particles described here may complement the scheme of atom guiding in hollow fibers [11,31,32], possibly improving the flux achievable within fibers when the fiber is bent. However, because we do not trap all particles, van der Waals interactions with the wall will reduce the transport efficiency. Also, if a buffer gas is present, transport by LID [33] must be taken into account. When LID is avoided, this process may also lead to particle separation when another species that is not strongly perturbed by the dipole force is introduced into the fiber. In this case, a pressure differential will not be produced because the unperturbed species will move in the opposite direction compensating for the transport of polarizable atoms that are pushed in the direction of the travelling wave. For a large detuning, this force will dominate over LID, and like LID, separation along the fiber will occur. Such a scheme may be used to separate atoms or molecules as in the manner of a gas chromatograph that is based on the polarizable interactions of atoms or molecules with light, rather than with the interactions of polar molecules with the wall of a capillary.

The drift velocity calculated above can only be sustained for a short period of time in a closed system until the pressure difference created equals the effective pressure induced by the dipole force. This pressure can be estimated by assuming that the pressure gradient is equal to the macroscopic dipole force per unit volume, which can be calculated from the initial momentum flux $0.5MV_{dr}N/\tau_{\mathrm{col}}$. The pressure difference across the fiber is given by $\Delta p \approx 0.5MV_{dr}NL/\tau_{\mathrm{col}}$, where L is the length of the fiber. A maximum pressure difference of 0.013 Pa or 95 μTorr is obtained for a 3 cm length fiber at the 560 K conditions calculated above. This pressure difference could, for example, be measured by a differential capacitance manometer which is capable of measuring pressure differentials to at least an order of magnitude below this value.

IV. CONCLUSIONS

We have predicted a range of new phenomena that result from optical Landau damping. These include the creation of bulk drift in a gas subject to optical potential as well as a measurable damping of optical field within an optical cavity. We have studied these processes for periodic optical potentials (lattices), whose well depth is less than the average kinetic energy of gas particles. For relatively large optical periodic potentials (100s of K) created by pulsed optical fields, we have predicted drift velocities in the 10 m/s range, while for weaker (1 mK) CW potentials we have predicted a bulk drift in a fiber which leads to the establishment of a pressure difference induced by the optical potential across a capillary. By studying the dissipation of the optical potential in a cavity which contains a high-density gas, we shown that the Landau damping of the optical potential could be measured by a change in the cavity decay rate which is dependent on the velocity of the potential and the width of the thermal distribution function.

[1] L. D. Landau, Zh. Eksp. Teor. Fiz. **16**, 949 (1955).
[2] B. B. Kadomtsev, *Collective Phenomena in Plasmas* (Pergamon Press, New York, 1982).
[3] F. F. Chen, *Introduction to Plasma Physics and Controlled Fusion, Volume 1, Plasma Physics*, 2nd ed. (Plenum Press, New York, 1984).
[4] S. Habib, H. E. Kandrup, and P. F. Yip, Astrophys. J. **309**, 176 (1986).
[5] I. Lerche and R. Schlickeiser, Astron. Astrophys. **366**, 1008 (2001).
[6] B. Jackson and E. Zaremba, New J. Phys. **5**, 88 (2003).
[7] N. J. Fisch, Rev. Mod. Phys. **59**, 175 (1987).
[8] M. Schiffer, M. Rauner, S. Kuppens, M. Zinner, K. Sengstock, and W. Ertmer, Appl. Phys. B: Lasers Opt. **67**, 705 (1998).
[9] J. D. Miller, R. A. Cline, and D. J. Heinzen, Phys. Rev. A **47**, R4567 (1993).
[10] D. M. Stamper-Kurn, M. R. Andrews, A. P. Chikkatur, S. Inouye, H. J. Miesner, J. Stenger, and W. Ketterle, Phys. Rev. Lett. **80**, 2027 (1998).
[11] M. J. Renn, D. Montgomery, O. Vdovin, D. Z. Anderson, C. E. Wieman, and E. A. Cornell, Phys. Rev. Lett. **75**, 3253 (1995).
[12] F. L. Moore, J. C. Robinson, C. F. Bharucha, B. Sundaram, and M. G. Raizen, Phys. Rev. Lett. **75**, 4598 (1995).
[13] S. R. Wilkinson, C. F. Bharucha, M. C. Fisher, K. W. Madison, P. R. Morrow, Q. Niu, B. Sundaran, and M. G. Raizen, Nature (London) **387**, 575 (1997).
[14] D. A. Steck, W. H. Oskay, and M. G. Raizen, Science **293**, 274 (2001).
[15] H. Stapelfeldt, H. Sakai, E. Constant, and P. B. Corkum, Phys. Rev. Lett. **79**, 2787 (1997).
[16] J. Karczmarek, J. Wright, P. Corkum, and M. Ivanov, Phys. Rev. Lett. **82**, 3420 (1999).
[17] D. M. Villeneuve, S. A. Aseyev, P. Dietrich, M. Spanner, M. Y. Ivanov, and P. B. Corkum, Phys. Rev. Lett. **85**, 542 (2000).
[18] R. W. Boyd, *Nonlinear Optics* (Academic Press, Boston, 1992).
[19] R. Fulton, A. Bishop, M. N. Shneider, and P. F. Barker (unpublished).
[20] P. F. Barker and M. N. Shneider, Phys. Rev. A **64**, 033408 (2001).
[21] P. F. Barker and M. N. Shneider, Phys. Rev. A **66**, 065402 (2002).
[22] M. N. Shneider and P. F. Barker, Proc. SPIE **5448**, 193 (2004).
[23] P. Bhatnagar, E. P. Gross, and M. Krook, Phys. Rev. **94**, 511 (1954).
[24] D. A. Anderson, J. C. Tannehill, and R. Fletcher, *Computational Fluid Mechanics and Heat Transfer* (Hemisphere Publishing Corp., New York, 1984).
[25] http://www.lgrinc.com/products/nirmirrors.html
[26] J. J. Scherer, J. B. Paul, A. O'Keefe, and R. J. Saykally, Chem. Rev. (Washington, D.C.) **97**, 25 (1997).
[27] Yu. P. Raizer, *Gas Discharge Physics* (Springer-Verlag, Berlin, 1991).
[28] H. J. Metcalf and P. van der Straten, *Laser Cooling and Trapping* (Springer-Verlag, New York, 1999).
[29] W. A. Hamel, A. D. Streater, and J. P. Woerdman, Opt. Commun. **63**, 32 (1987).
[30] E. A. J. Marcatile and R. A. Schmeltzer, Bell Syst. Tech. J. **43** 1783 (1964).
[31] R. G. Dall, M. D. Hoogerland, K. G. H. Baldwin, and S. J. Buckman, J. Opt. B: Quantum Semiclassical Opt. **1**, 396 (1999).
[32] M. J. Renn, A. A. Zozulya, E. A. Donley, E. A. Cornell, and D. Z. Anderson, Phys. Rev. A **55**, 3684 (1997).
[33] F. Kh. Gel'mukhanov and A. M. Shalagin, JETP Lett. **29**, 7111 (1979).